

Mini review

Design and Applications of Ratiometric Electrochemical Biosensors

*Linlin Hou**, *Chunyan Duan* and *Panpan Ding*

Henan Province of Key Laboratory of New Optoelectronic Functional Materials, College of Chemistry and Chemical Engineering, Anyang Normal University, Anyang, Henan 455000, People's Republic of China

*E-mail: linlin9918@163.com

Received: 9 March 2019 / *Accepted:* 12 April 2019 / *Published:* 10 May 2019

Electrochemical biosensors have been used in the fields of disease diagnosis, environmental monitoring, and food safety. However, the traditional electrochemical biosensors have some shortcomings, such as poor stability and reproducibility. Ratiometric electrochemical biosensors can eliminate the potential interference, provide internal self-calibration, and improve detection sensitivity and selectivity. In this paper, the construction strategies for ratiometric electrochemical biosensors and their applications in biochemical analysis of proteins, nucleic acids, small biological molecules and metal ions are summarized.

Keywords: Ratiometric electrochemical biosensors; signal amplification

1. INTRODUCTION

The electrochemical biosensor is an analytical detection device based on ionic conductivity. As a non-mechanical sensing device, electrochemical biosensor based on the specific acceptor/target interaction has been developed to accurately determine biological or chemical targets. By making the target react electrochemically within the sensor, the measured molecule is consumed or a certain amount of electroactive substance is produced. Electrochemical biosensor has some outstanding qualities in measurement and operation. It has been widely used in clinical medical diagnosis, drug and food analysis and environmental detection [1-3]. The electrochemical biosensor commonly includes three components: sensitive identification element, signal conversion element and detection element. The commonly used identification elements are biomaterials and the signal conversion elements are electrodes [4]. The detection signals include potential, current or conductance. Based on the specific biomolecular recognition mechanism, the target molecule can be captured by the

recognition element (e.g. antigen, antibody, hormone or enzyme) attached on the electrode surface [5-10]. The recognition process is accompanied by electron transfer, leading to the change in electrochemical signal, such as voltage, current and impedance. Electrochemical biosensor can be divided into labeled or label-free formats. Label-free electrochemical biosensor could be operated easily with low false signal rate, but its detection sensitivity is low for the detection of biological molecules. The labeling process of labeled electrochemical biosensor is relatively complicated, but its sensitivity is relatively high. However, traditional single-label biosensor has inherent defects. Firstly, the single-labeled biosensor shows low sensitivity and can not be used to detect ultra-trace biomolecules. Secondly, the single-labeled biosensor is a “one-to-one” mode of electrical signal output; thus, positive or negative false recognition may cause the signal change. Compared with the traditional electrochemical biosensor, the ratiometric electrochemical biosensor using two electroactive substances to generate electrical signals at different potentials can achieve dual signal response in the same sensing system. The potential interference of the electrochemical signals generated by the inherent background can be effectively avoided by using the ratiometric strength analysis of the dual signals. Therefore, the ratiometric electrochemical biosensors have the built-in correction ability for the influence of electrical signals from the system itself or background, improving sensitivity and selectivity. Highly selective and sensitive ratiometric electrochemical biosensor becomes the ideal analytical tool for assay of target in complex detection system [11-13]. Such biosensor usually requires the use of two or more electroactive molecules to generate electrical signals. By analyzing the signal ratio of two electroactive molecules at different potentials, the analytical and detection can be carried out. The commonly used electroactive molecules are methylene blue (MB), ferrocene (Fc) and thionine (Thi) [14-17]. In recent years, various ratiometric electrochemical biosensors including dual-signal or multi-signal modes have been successfully constructed and showed a broad prospect of development. In this paper, the preparation strategies of ratiometric electrochemical biosensors and their applications are summarized.

2. STRATIES OF RATIOMETRIC ELECTROCHEMICAL BIOSENSORS

Ratiometric electrochemical biosensor determines the concentration of analyte according to the current ratio of two electrochemical signals, which improves the detection sensitivity and selectivity to a certain extent. Considering the response of electrochemical signal to analyte, the preparation strategies of ratiometric electrochemical biosensor can be divided into two categories: built-in reference signal and dual reference signal. For the traditional single-signal sensing strategy, the electrical signal varies singly with the concentration of analyte. For the dual-signal sensing strategy, ratiometric electrochemical biosensor can be designed with only one signal dependent on the content of analyte and another internal reference signal independent of the content of analyte. As to the dual reference signal, electrochemical signal is dependent on the content of analyte.

Ratiometric electrochemical biosensor based on built-in reference signal sensing strategy overcomes some shortcomings in improving the sensitivity and anti-interference and decreasing the detection limit by external environmental factors. By introducing redox an active substance (e.g. MB, Fc and Thi) as built-in reference, interference factors from instruments, testing environment and

samples can be eliminated. According to the built-in reference signal sensing strategy, electrochemical biosensors can be prepared by various signal transduction methods, but the strength of built-in reference signal should be kept constant when the analyte concentration changes. Based on the current ratio of response signal to internal reference signal as the measurement standard of analyte, the errors caused by micro-environment and other factors in the process of electrochemical sensing can be effectively reduced, which improving the sensitivity, repeatability and accuracy of ratiometric electrochemical biosensor. For example, Cai and co-workers prepared a ratiometric electrochemical immunosensor using the electrical signal generated by PTh-Au modified on the electrode surface as the built-in reference signal and the electrical signal generated by $K_3[Fe(CN)_6]$ in electrolyte as the detection signal [18]. The sensor can detect carcinoembryonic antigen (CEA, a tumor biomarker) in a linear range of 0.005 ~ 40 ng/mL with a detection limit of 2.2 pg/mL. When CEA was immobilized on the modified electrode by an immune reaction, it would hinder the electron transfer of $K_3[Fe(CN)_6]$ on the electrode and change the detection signal, while the reference signal produced by PTh-Au remains constant in this process. The CEA concentration can be accurately detected by analyzing the ratio between the detection signal and the internal reference signal.

The strategies of ratiometric electrochemical biosensor with dual reference signal are mainly based on the change of the distance between the two electroactive markers and the electrode surface before and after the capture of target. The sensing strategies can not only improve the detection sensitivity, but also avoid the interference which is independent of the analyte concentration, such as the change of electrode area and the non-specific adsorption. Using the ratio of two electroactive molecules on the electrode surface as the output signal, the signal change caused by complex samples can be reduced, and the reproducibility and stability can be improved.

3. APPLICATIONS OF RATIOMETRIC ELECTROCHEMICAL BIOSENSORS

At present, the ratiometric electrochemical biosensors have been widely used in the analysis and detection of proteins, nucleic acids, metal ions and other small biological molecules. These reported works are summarized herein based on the difference of targets.

3.1 Proteins

To date, ratiometric electrochemical biosensors have been successfully applied to the detection of tumor markers CEA, prostate specific antigen (PSA), thrombin, prion protein and proteases. They show high selectivity as well as sensitivity, and good stability [18-31]. For example, Cai and co-workers reported an accurate, reliable and sensitive electrochemical immunosensor for tumor marker ratiometric assay by a ratiometric method. CEA was used as the model analyte [18]. The immunoassay was carried out by a simple expedient way. $K_3[Fe(CN)_6]$ in electrolyte was the indicator signal. Polythionine-gold (PTh-Au) modified on the electrode surface acted an internal reference signal. The signal of $K_3[Fe(CN)_6]$ changed once the CEA was attached onto the electrode by the antibody-antigen interaction. In this process, no change was observed for the internal reference signal at a given pH. The content of CEA was thus determined by the ratio between the current of $K_3[Fe(CN)_6]$ and PTh-Au with

a detection limit of 2.2 pg/ml and a good specificity in the linear range from 0.005 ng/mL to 40 ng/mL. Gao and co-workers designed a dual-signal ratiometric electrochemical aptamer biosensor to detect thrombin by self-assembly of target catalytic cyclic hybridization [20]. The sensor contains two DNA hairpin structures: H1 and H2. The 3'-end of hairpin structure H1 having a thrombin-binding sequence was modified with Fc, which can pair with another complementary sequence to form a hairpin structure without thrombin. The 3'-end label of hairpin H2 has MB and a complementary sequence with H1 sequence. H2 was modified on the electrode surface to make MB close to the electrode and produce strong electrochemical signal. Because H1 contains thrombin adaptation sequence, the addition of thrombin can open H1 hairpin structure, expose the complementary part of H1 and H2 sequence, and promote the hybridization between H1 and H2 on the electrode surface. H2 can displace and release target protein from H1 through DNA branching migration. Consequently, Fc tag was close to the electrode surface and MB tag was far away from the electrode surface. This led to the change in the electrochemical signals of MB and Fc. The released target protein continued to open another H1, thus triggering the above cycle. The dual-signal ratiometric biosensor using I_{Fc}/I_{MB} as the response signal showed high sensitivity and repeatability. The detection range is 0.1 pM ~ 10 nM, and the detection limit is 41 fM. The biosensor has high selectivity for thrombin detection. The determination of thrombin was not disturbed in the presence of other biological molecules, such as immunoglobulin G (IgG), adenosine triphosphate (ATP) and human serum albumin (HSA). Ren and co-workers have developed a ratiometric electrochemical sensing strategy for one-step determination of protein biomarkers [32]. The Fc-labeled hairpin DNA was immobilized on the surface of the gold electrode to obtain the sensing interface. In the presence of DNA-antibody 1 (DNA 1-Ab1) and DNA 2-antibody 2 (DNA 2-Ab2) probes labeled by MB, the addition of target protein can induce sandwich immune reaction between the two probes, trigger the hybridization of DNA 1 and DNA 2, open the hairpin DNA on the electrode surface, and produce three-arm DNA structures on the sensor surface. This DNA assembly made the release of Fc from electrode and facilitated the approaching of MB to the electrode, thus causing the change in the electrical signals of both Fc and MB. The detection limit of this method for PSA detection is 4.3 pg/mL, and the linear range is 0.01 ~ 200 ng/mL. By changing the antibodies linked by affinity probes, this strategy can be applied to the detection of other proteins.

Yu and co-workers constructed a ratiometric electrochemical biosensor for the detection of prion protein based on the host-guest competition strategy [29]. Using host-guest interaction between β -cyclodextrin (β -CD) and MB, they introduced MB-labeled prion protein aptamer (MB-Apt) onto a glassy carbon electrode modified by multi-walled carbon nanotube-beta-cyclodextrin (MWCNTs- β -CD). In the presence of prion, MB-Apt located in the inner cavity of β -CD is replaced by ferrocene carboxylate (FcA), which made FcA close to the electrode surface to produce a large oxidation peak current from FcA. The interaction of prion protein with MB-Apt forms a biogate, blocking the β -CD lumen and preventing FcA from entering the lumen by the replacement reaction. This resulted in the increase of the oxidation current of MB and the decrease of the current of FcA. The sensor has good selectivity to target protein, and the detection limit is down to 160 fM. Recently, Zhu and co-workers developed a dual-signal ratiometric strategy for highly sensitive assay of proteins with the DNA walker strategy. In their strategy, thrombin was chosen as a model [31]. Firstly, the DNA walkers (DWs) and the thrombin aptamer (TBA) hybridized to produce a double-stranded DNA. The double-

stranded DNA and MB-labeled DNA (MB-DNA) were attached onto the AuNPs-modified electrode. In the presence of Fc-DNA, MB-DNA hybridized with Fc-DNA to form a MB-DNA/Fc-DNA duplex. With the addition of TB, DWs were released because of the specific interactions between TB and TBA. The released DWs were then hybridized with one part of Fc-DNA in MB-DNA/Fc-DNA duplex, thus inducing the formation of a duplex at the 3'-termini of Fc-DNA. This triggered the Exo III cleavage process and the removing of Fc from the electrode and the releasing of DWs. The DWs were hybridized again with another Fc-DNA, thus performing the DNA walker recycling process. The remained single-stranded MB-DNA formed a hairpin structure in the presence of Mg^{2+} because of its tailor-made complementary bases at both ends. This resulted in an enhancement of MB signal (I_{MB}) and a decrease of Fc signal (I_{Fc}). the proposed electrochemical aptasensor showed superior analytical performances for sensitive assay of thrombin with a linear range of 0.1 pM ~ 10 pM and a low detection limit of 56 fM by measuring the value of I_{MB}/I_{Fc} .

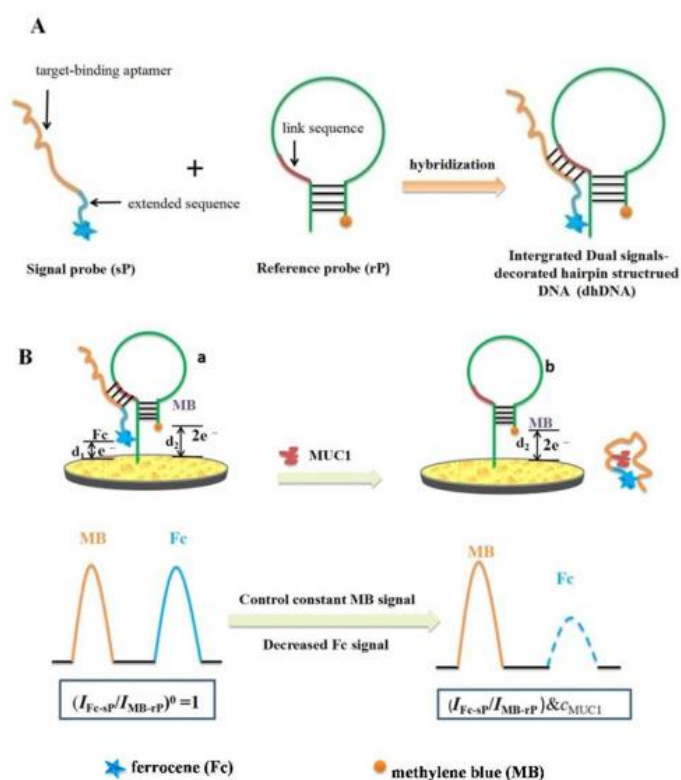


Figure 1. (A) Schematic representation of the formation of dhDNA that serves as an electrochemical ratiometric probe; (B) Detection mechanism of the biomarker based on this dhDNA ratiometric probe, which is illustrated by the state of dhDNA/AuNPs/GCE before (a) and after (b) introduction of MUC1. Reprinted with permission from reference [19]. Copyright 2017 American Chemical Society.

The universality provided a great potential in biosensing, biomedical research, and clinical diagnosis. Moreover, Peng and co-workers developed an amplified electrochemical ratiometric aptasensor for nuclear factor kappa B (NF- κ B) assay based on target binding-triggered ratiometric signal readout and polymerase-assisted protein recycling amplification strategy [23]. Yang and co-workers reported three-dimensional graphene-based ratiometric signal amplification aptasensor for

highly sensitive and selective detection of mucin1 (MUC1) [17]. Deng and co-workers also proposed a ratiometric electrochemical method for MUC1 detection (Figure 1) [19]. Combining Fc-labeled signal probe (Fc-sp) and MB-modified internal reference probe (MB-rP), a double signal-labeled hairpin-structured DNA (dhDNA) ratiometric probe was designed. The aptasensor is feasible to detect MUC1 through one-step incubation procedure. The dhDNA ratio probe exhibited a strong ability to eliminate the interference induced by environmental change.

Very recently, Lin and co-workers reported a satisfactory biosensing platform to improve the binding efficiency of antigenic proteins and antibodies using DNA tetrahedral nanostructures (DTNs) as the carriers of stable reference signal (Figure 2) [22]. Tris-(4,4'-dicarboxylicacid-2,2'-bipyridyl) ruthenium (II) dichloride ($\text{Ru}(\text{dcbpy})_3\text{Cl}_2$) (an electrochemiluminescence (ECL) reagent) was modified on the electrode through the formation of classical sandwich complex of antibody-antigen-antibody. dsDNA on both sides of DTN were used as the carrier of MB to generate stable electrochemical internal reference signal to correct the potential interference. However, the ECL response was enhanced with the increase of target Golgi protein 73 (GP73) concentration. Based on the ratio of ECL signal of $\text{Ru}(\text{dcbpy})_3\text{Cl}_2$ to electrochemical signal of MB, an immunosensor with high selectivity and reproduction was developed. The ratio was linear with the concentration of GP73 in the range of 15 $\mu\text{g}/\text{mL}$ to 0.7 ng/mL , and the detection limit was 15 pg/mL .

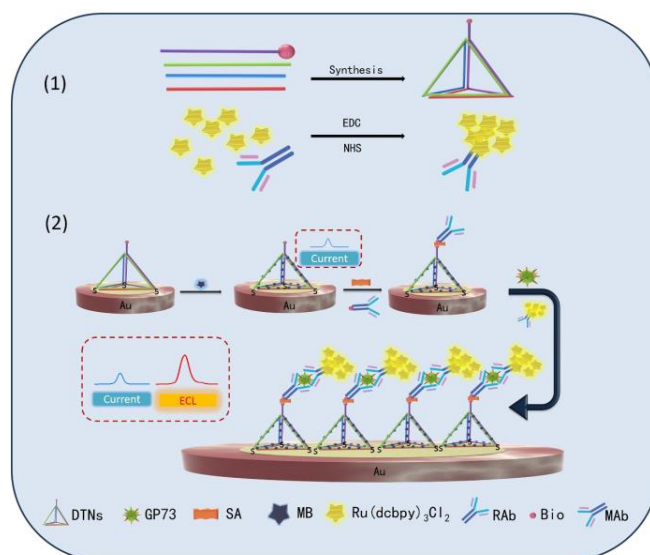


Figure 2. Schematic diagram of ratiometric ECL immunosensor for GP73. Reprinted with permission from reference [22]. Copyright 2019 American Chemical Society.

3.2 Nucleic acids

Nucleic acid detection plays an important role in environmental monitoring as well as early diagnosis and prognosis judgement of diseases [33]. Ratiometric electrochemical biosensors have been used for simple, rapid and ultra-sensitive detection of nucleic acids [34-46]. For example, Cui and co-workers have developed a ratiometric electrochemical biosensor based on DNA four way structure (DNA-4WJ) and enzyme-assisted cyclic amplification [34]. The sensor consists of a three-stranded

molecular beacon (THMB) assembled on the electrode and two unmodified auxiliary DNA sequences (α and β sequences). THMB consisting of MB-labeled hairpin probe (HP) and Fc-labeled nucleotide sequence (UT) is fixed on the electrode surface by UT. The hairpin structure of HP made MB close to the electrode surface, thus producing strong electrochemical signal; while the expansion of UT configuration caused Fc far from the electrode surface to produce weak electrochemical signal. Because each of the two auxiliary DNA sequences contained a complementary sequence of HP and a complementary sequence of target DNA, target DNA and two auxiliary DNA hybridized with HP to form DNA-4WJ structure, thus destroying the THMB structure. This promoted MB to be far away from the electrode surface and Fc to be close to the electrode surface, resulting in the decrease of MB electrochemical signal and the increase of Fc electrochemical signal. The concentration of target DNA can be determined by the ratio of the two electrochemical signals of MB and Fc. The digestion of DNA-4WJ structure by RNase HIII can induce the release of HP and auxiliary DNA sequence, triggering the next cycle and amplifying the enzyme-assisted signal cycle. The ratiometric electrochemical sensor has the advantages of simple preparation and high sensitivity. The detection range is 0.1 pM ~ 100 nM, and the detection limit is down to 0.063 pM. In addition, the introduction of DNA-4WJ structure benefited the high selectivity for target DNA.

Xiong and co-workers have developed a ratiometric electrochemical DNA biosensor for the sensitive detection of target DNA based on the exonuclease III (Exo III)-assisted target recycling amplification strategy (Figure 3) [43]. The stem ring (hairpin) DNA capture probe (HP) was labeled with MB at the 3'-protrusion end and with Fc at the middle of the ring. T-DNA triggered the division of exon III by hybridizing with HP, which is accompanied by the release of T-DNA. The results demonstrated that the MB tag is far from the electrode surface and the Fc tag is close to the electrode surface, which resulted in the decrease of MB peak current and the increase of Fc peak current. The value of I_{Fc}/I_{MB} was linear with the concentration of T-DNA from 0.01 pM ~ 0.8 pM. The detection limit of 4.16 fM is much lower than that of achieved by the reported electrochemical DNA biosensor. Recently, Xiong and co-workers also developed a ratiometric electrochemical DNA biosensor based on the triple-helix molecular switch (Figure 4) [38]. Firstly, a hairpin MB-DNA capture probe was assembled on the electrode surface. After that, DNA labeled with Fc at two ends (Fc-DNA) hybridized with MB-DNA, resulting in the formation of the triple-helix structure. In the presence of HIV-1 gene target DNA (T-DNA), Fc-DNA hybridized with T-DNA. This made the triple-helix stem disassembled and allowed for the recovery of hairpin structure of MB-DNA. Finally, when the MB label was close to the electrode, the Fc label diffused from the electrode surface, leading to the decrease in the peak current of Fc and the increase in the peak current of MB (I_{MB}). The linear relationship between I_{MB}/I_{Fc} and T-DNA concentration was 0.5 ~ 80 pM. The detection limit was down to 0.12 pM. In addition, the biosensor can be easily regenerated with an alkaline buffer containing Mg^{2+} without thermal annealing.

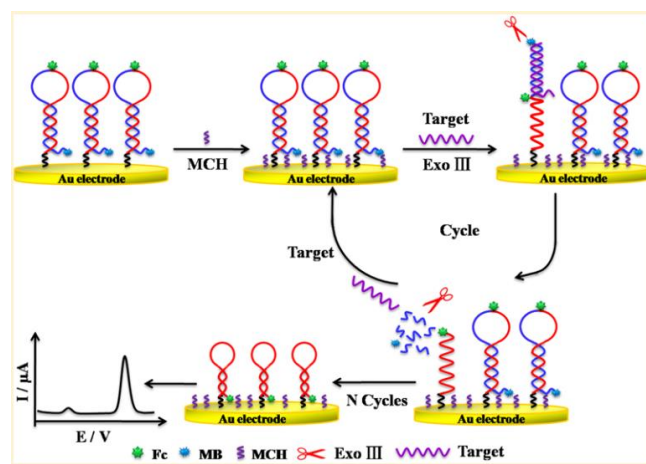


Figure 3. Schematic illustration of the electrochemical biosensor for target DNA detection. Reprinted with permission from reference [43]. Copyright 2015 American Chemical Society.

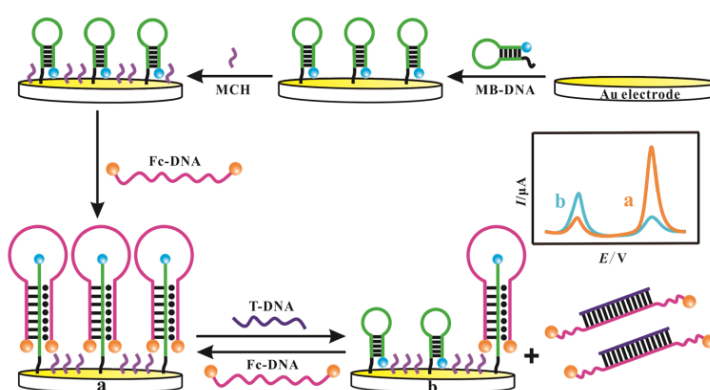


Figure 4. Schematic Diagram of the E-DNA Biosensor for the Detection of T-DNA. Reprinted with permission from reference [38]. Copyright 2017 American Chemical Society.

MiRNAs are closely related to the occurrence and development of tumors and other diseases. They have been considered as important markers for clinical diagnosis [47-49]. Zhang's group have developed a ratiometric electrochemical biosensor based on biped DNA walkers to detect miRNA-21 in cancer cell exosomes [37]. The DNA "walker" consists of two parts of "foot" sequence and a part of "body" sequence, which can hybridize with complementary DNA strand modified on magnetic beads through "body" sequence. Its trajectory is MB-labeled hairpin DNA (MB-H1) modified on the electrode surface. The targets (miRNA-21) made DNA "walkers" released from the magnetic bead. The resulted DNA "walkers" continued to walk along DNA tracks, opening the MB-H1 hairpin structure and exposing its sticky ends. When Fc-labeled hairpin DNA (Fc-H2) was added, a double strand was formed by crossing MB-H1 with viscous terminal mediated chain displacement reaction (TMSDR), releasing DNA "walker" and starting the next cycle. Multiple cycles lead to the increase of Fc content on the electrode surface, while no change occurred between MB (a built-in reference signal molecule) and electrode. The method can detect miRNAs sensitively by measuring the current signal ratio. The linear range is from 0.1 fM ~ 100 fM, and the detection limit reaches to 67 aM. The biosensor can be used to detect miRNAs in breast cancer cell lines and serum. Yuan and co-workers

have proposed a ratiometric electrochemical biosensor based on duplex-specific nuclease (DSN) double-signal amplification for the detection of miRNAs [36]. The Fc-labeled hairpin capture probe (CP) was modified on the gold electrode to obtain the sensing interface. The target miRNA hybridized with CP probe and opened the hairpin structure of CP to form a double strand of miRNA-DNA. The DNA strand in the double strand of miRNA-DNA was cut by DSN, which releasing the target miRNA, and triggering the next round of shearing process. This caused a large number of Fc tags leaving the electrode surface along with the DNA strand shearing, thus decreasing the electrical signal of Fc. The remained DNA fragments on the electrode can be used as the primers for hybridization chain reaction (HCR). With the addition of two other single strands of DNA (HDNA and HDNA'), the composite of DNA/AuNPs/Thi was captured to form double-stranded DNA aggregate. This resulted in an increase of electric signal due to the aggregation of a large number of Thi molecules on the electrode surface. This method can selectively detect miRNA-141 by analyzing the change of current ratio between Fc and Thi ($I_{\text{Thi}}/I_{\text{Fc}}$). The detection range is 0.1 fM ~ 100 pM, and the detection limit is 11 aM. Moreover, Ge and co-workers have developed a novel affinity-mediated ratiometric electrochemical biosensor for miRNA quantification (Figure 5) [39]. The 1-naphthalenesulfonate diazonium salt was electrochemically grafted onto the surface of ITO electrode for the first time. The modified electrode exhibited excellent discrimination ability for ssDNA and dsDNA. The realization of miRNA detection lies in a compatible design of T7 nucleic acid exonuclease-assisted isothermal amplification method. In this work, the target miRNA triggered the continuous and reverse affinity reversal of two electrochemical signal reporters, MB-labeled hairpin reporter and Fc-labeled dsDNA reporter. By measuring the obvious change of peak current intensity ratio of Fc and MB, the electrochemical biosensor showed a sensitive detection limit of 25 aM. In addition, the proportional biosensor platform has high sensitivity to let-7a miRNA and can effectively distinguish miRNA family members.

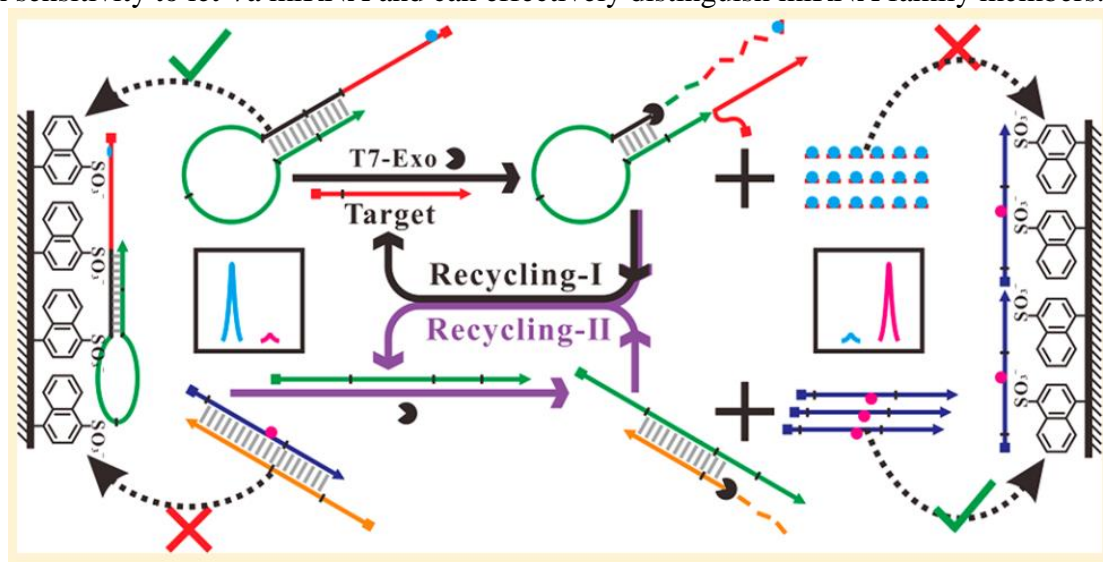


Figure 5. Schematic illustration of the design principle for the amplified ratiometric homogeneous electrochemical biosensing of miRNA on the NS-ITO electrode. Reprinted with permission from reference [39]. Copyright 2017 American Chemical Society.

Gai and co-workers have constructed a new label-free and enzyme-free ratiometric electrochemical miRNA biosensor based on target-triggered Ru(III) release and redox recycling (Figure 6) [40]. $[\text{Ru}(\text{NH}_3)_6]^{3+}$ was ingeniously inserted in the pore of positively charged mesoporous silica nanoparticle (PMSN). $[\text{Fe}(\text{CN})_6]^{3-}$ in solution was used to facilitate Ru(III) redox recycling in view of its distinctly separated reduction potential and different redox property. Due to the liberation of the generated RNA/ssDNA complex from PMSN, the target miRNA triggered the release of $[\text{Ru}(\text{NH}_3)_6]^{3+}$ and triggered the redox reaction of $\text{Ru}(\text{II}) + \text{Fe}(\text{III}) \rightarrow \text{Ru}(\text{III}) + \text{Fe}(\text{II})$ with Fe(III). With the release of $[\text{Ru}(\text{NH}_3)_6]^{3+}$ and the consumption of Fe(III), an enhancement in the current ratio of $[\text{Ru}(\text{NH}_3)_6]^{3+}$ to $[\text{Fe}(\text{CN})_6]^{3-}$ ($I_{\text{Ru(III)}}/I_{\text{Fe(III)}}$) was obtained. The ratio is dependent upon the target concentration. Furthermore, the detection limit of the method was down to 33 aM (S/N = 3), which is comparable or even lower than that obtained by other methods reported in literatures.

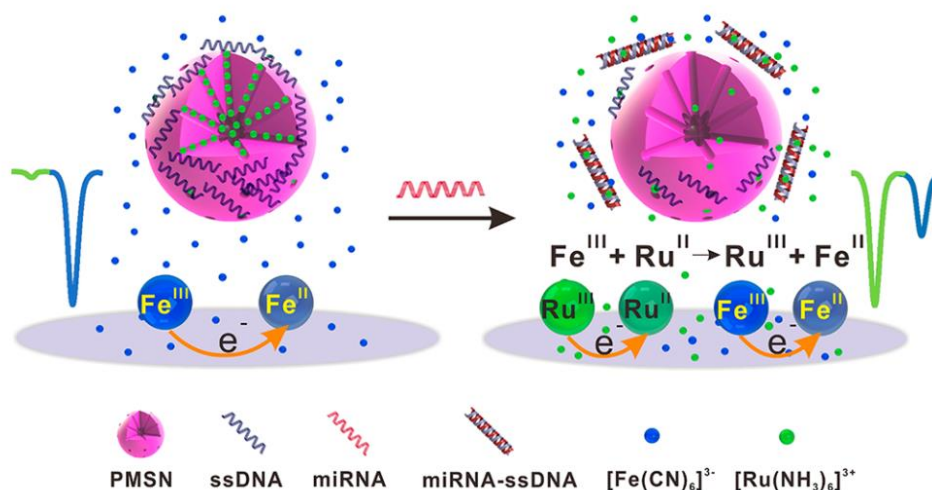


Figure 6. Schematic principle of the ratiometric homogeneous electrochemical miRNA biosensor. Reprinted with permission from reference [40]. Copyright 2017 American Chemical Society.

3.3 Small biological molecules

Small biological molecules, such as ascorbic acid (AA), dopamine, bisphenol A (BPA), adenosine, hydrogen peroxide, H_2S and so on, play an important role in human metabolism and life activities [50]. For example, AA is an indispensable nutrient and antioxidant in human body. It can protect human body from the threat of free radicals and plays a key role in many physiological and pathological processes. A few of ratiometric electrochemical biosensors have been developed recently for the detection of small biological molecules [28, 30, 51-64]. Chen and co-workers have designed a ratiometric electrochemical sensor for in vivo selective and reliable detection of cerebral AA in the brain of living rats (Figure 7) [55]. Carbon black (Ketjen black, KB) is used as electrode material because of its good conductivity, high surface area ratio and low cost. In this work, the redox probe thionine was assembled on KB to form thionine/KB nanocomposites by hydrophobic and π - π stacking interactions. A specific electrochemical sensor for AA detection was prepared by coating the nanocomposites on the electrode surface. The functionalized nanocomposites effectively promoted AA

oxidation at the potential of -0.14 V. At -0.22V, a pair of well-defined redox waves can be used as an appropriate internal reference for AA detection. This method was also successfully applied for the selective detection of AA in rat brain. Moreover, Wang and co-workers constructed a ratiometric electrochemical biosensor to determine AA using metal-organic framework materials of PCN-333 (Al) [52]. KB for the catalytic oxidation of AA was encapsulated into the hole of PCN-333 (Al) modified on glassy carbon electrode. Thi was chosen as internal reference signal molecule. KB in PCN-333 (Al) can catalyze the oxidation of AA to produce oxidation peak current, while the built-in reference signal produced by Thi remains unchanged. The current ratio between them has been used to achieve the sensitive detection of AA. The detection range of the biosensor is 14.1 ~ 5.5 mM, and the detection limit is 4.6 mM. The porous structure of PCN-333 (Al) can effectively fix KB and Thi and avoid the adhesion or aggregation of KB and Thi on the electrode surface, thus improving the stability of the sensor. Moreover, PCN-333 (Al) facilitated the accumulation of analytes into the pore to improve detection selectivity.



Figure 7. Schematic illustration of rationally designed ratiometric electrochemical sensor for selective and reliable measurement of cerebral AA in living brains. Reprinted with permission from reference [55]. Copyright 2017 American Chemical Society.

Cui and co-workers have developed a ratiometric electrochemical biosensor for adenosine detection based on the interaction between MB and A-T base sequences [51]. Capture probe DNA modified with MB at the 3'-terminal thymine (T) base was fixed on the electrode surface. Meanwhile, the Fc-labeled aptamer was designed to recognize adenosine. In the absence of adenosine, these two DNA chains partially complement each other, making MB far from the electrode surface and Fc close to the electrode surface. This resulted in a smaller peak current ratio (I_{MB}/I_{Fc}). Once adenosine formed a G-tetrad structure with Fc-labeled aptamer chain, the aptamer chain would leave the electrode surface. This made Fc away from the electrode surface and MB close to the electrode surface, resulting in the increase in the I_{MB}/I_{Fc} value. The detection limit of the method for adenosine is 90.8 pM with a linear range of 0.1 nM ~ 100 μ M.

Hydrogen peroxide (H_2O_2) is a multifunctional biomarker widely involved in enzymatic catalysis, cell signal transduction and other processes. It is the precursor of active hydroxyl radicals and other reactive oxygen species involved in the oxidative stress process to cause various diseases. Goggins and co-workers have synthesized borate ester-ferrocene derivatives as H_2O_2 probes [60],

which showed a peak oxidation current at a voltage of 0.05 V. H_2O_2 can oxidize the probe and promote the hydrolysis of borate esters, leading to the formation of ferrocene aminobenzene. The oxidation current peak of borate ester-ferrocene derivatives decreased at 0.05 V, and the oxidation peak current of ferrocene aminobenzene derivatives increased gradually at -0.2 V. The ratiometric electrochemical detection of H_2O_2 can be carried out by measuring the peak current of ferrocene and borate ester-ferrocene derivatives. The linear detection range is 0 ~ 800 μM .

Hydrogen sulfide (H_2S) is a gas transmitter in the biological system, which can regulate cardiovascular, neuronal and immune systems. Abnormal H_2S levels are associated with many diseases, such as chronic kidney disease, cirrhosis and Down's syndrome. Manibalan and co-workers have synthesized two kinds of H_2S probes containing azide initiator group and reporting group (ABFC and NABFC) [57]. Real-time quantitative detection of H_2S released from living cells was realized. In the absence of H_2S , both probes exhibited a peak current at 0.23 V. H_2S can specifically trigger the release of two reporter groups: aminoferrocene (FA) and N-alkyl aminoferrocene (NFA), producing new peak currents at -0.06V and -0.1V, respectively. By analyzing the signal ratio of the two peak currents, H_2S can be specifically determined with a detection limit of 0.32 μM and 0.076 μM , respectively. Moreover, Shen and co-workers have developed a specific electrochemical strategy for the detection of lipopolysaccharides (LPS) using copper-based metal-organic frameworks (Cu-MOFs) as catalysts to trigger secondary cycle signal amplification (Figure 8) [58].

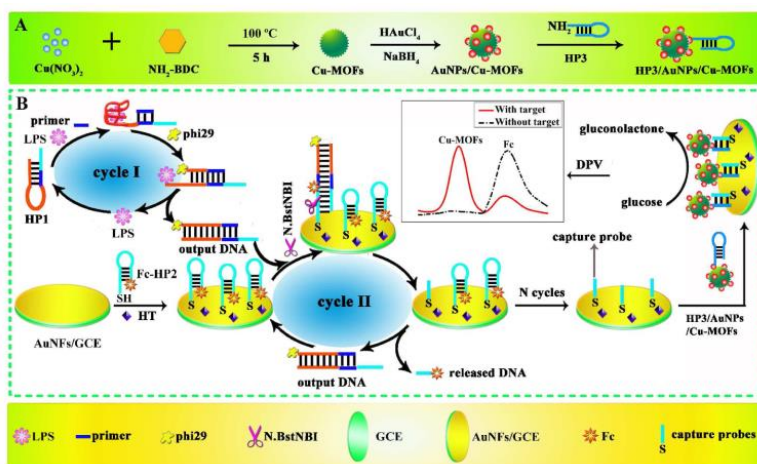


Figure 8. Schematic illustration of the fabrication of the aptasensor: (A) Preparation procedure of HP3/AuNPs/Cu-MOFs; (B) Signal amplification strategy and the detection principle for LPS. Reprinted with permission from reference [58]. Copyright 2015 American Chemical Society.

First, in the presence of target LPS, the conformational change of the hairpin probe 1 (HP1) triggered target cyclic induction polymerization with the assistance of phi29 DNA polymerase to produce output DNA. Then, the output DNA was hybridized with Fc-labeled hairpin probe 2 (Fc-HP2) to generate a cleavage site of endonuclease (N.BstNBI). In the presence of N.BstNBI, the original signal molecule of Fc was separated from the electrode. The hairpin probe 3 on the AuMPs-functionalized Cu-MOFs (HP3/AuNPs/Cu-MOFs) was hybridized with capture probe for hairpin assembly. In this paper, AuNPs/Cu-MOFs were used as the nanocarriers for the immobilization of HP3

and as the active materials for signal output. The cleavage site of Fc-HP2 was cleaved by the proposed target to trigger the secondary cycle. The capture probe was hybridized with HP3/AuNPs/Cu-MOFs, resulting in the decrease of the Fc signal. Then, the closing of Cu-MOFs to the electrode surface increased the signal. The biosensor had a detection limit of 0.33 fg/mL for LPS detection, and exhibited a wide linear range (1.0fg/mL ~ 100 ng/mL).

4.4 Metal ions

Accurate determination of metal ions (such as Cu^{2+} , Cd^{2+} and Hg^{2+}) is very important in the fields of biology, medicine, environment and chemistry. Many ratiometric electrochemical biosensors have been reported for the detection of metal ions [65-75]. For example, Hg^{2+} in the environment can cause serious damage to the physiological system and cause many acute and chronic diseases. Jia and co-workers have developed a ratiometric biosensor for Hg^{2+} detection by the formation of Y-DNA configuration [65]. DNA probe labeled with MB and Fc immobilized on gold electrode can form a Y-type DNA structure. Because Fc is close to the electrode and MB is far from the electrode, strong Fc signal and weak MB signal were obtained. Hg^{2+} can form stable T- Hg^{2+} -T complex with T-T mismatch base pairs in Y-type DNA structure, and transform Y-type DNA structure into hairpin structure. During the conversion process, the peak current of MB increased by approaching to the electrode surface, and that of Fc far from the electrode surface decreased. The detection range was 1 nM ~ 5 mM, and the detection limit was 0.094 nM. The specific binding between Hg^{2+} and T-T mismatch base pairs ensured the good selectivity of the biosensor. By the coordination of L-cysteine with Hg^{2+} , the Y-DNA structure on the electrode surface can be restored and the sensor can be regenerated.

Cu^{2+} is involved in regulating bone formation, cell respiration and connective tissue development. High concentration of Cu^{2+} has toxic and side effects on biological tissues [76]. Yu and co-workers have constructed a ratiometric biosensor for the detection of Cu^{2+} in rat brain using dihydroxy functional aggregated ionic liquids (DHF-PIL) as catalysts [66]. The macroporous structure of DHF-PIL provided a high surface area for the full loading of biomolecules. DHF-PIL was modified with built-in reference signal molecule of 2,2'-azadiazole (3-ethylbenzothiazoline-6-sulfonate) (ABTS) and Cu^{2+} -specific recognition molecule neurokinin B (NKB) by electrostatic interaction. NKB can specifically bind Cu^{2+} to form Cu^{2+} -(NKB)₂ complex and produce an oxidation peak current, while the signal of internal reference was constant during the whole process. The detection limit of Cu^{2+} is 0.24 μM , and the linear detection range is 0.9 ~ 36.1 μM . Moreover, Zhang and co-workers have developed a ratiometric electrochemical biosensor with Cu^{2+} as a model (Figure 9) [69]. First, the specific molecule, 2,2',2''-(2,2',2''-nitriлотris(ethane-2,1-diyl)-tris((pyridin-2-ylmethyl) azanediyl) triethanethiol (TPAASH), was designed and synthesized for specific recognition of Cu^{2+} . Meanwhile, electroactive molecule, 6-(ferrocenyl) hexanethiol (FcHT) was co-immobilized with TPAASH at the electrode surface as the inner reference molecule to provide a built-in correction for avoiding the environmental effect. The reduction peak of Cu^{2+} on the TPAASH-functionalized electrode was observed at -0.12 V. The high sensitivity is ascribed to the electro-catalytic activity of gold flower nanostructure.

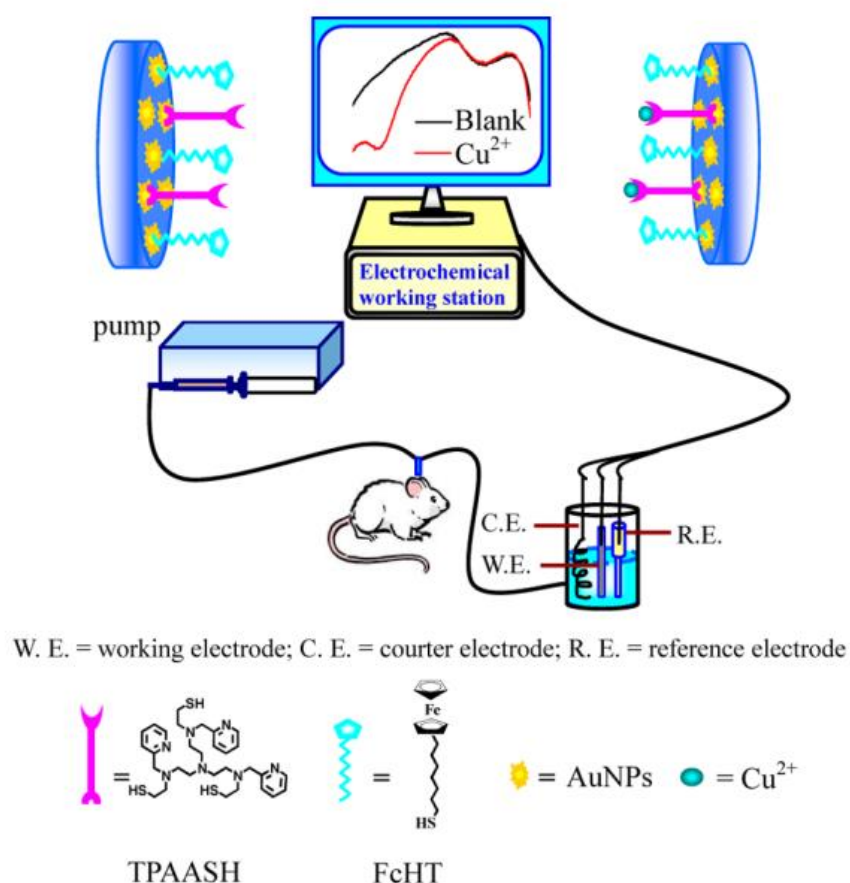


Figure 9. Schematic illustration of the ratiometric sensor for monitoring of Cu²⁺. Reprinted with permission from reference [69]. Copyright 2015 American Chemical Society.

Luo and co-workers designed a ratiometric biosensor to detect the content of Cu²⁺ and γ -cysteine (CySH) in the brain of living rats using a built-in reference signal (Figure 10) [67]. The detection system consisted of AuNPs-modified carbon fiber microelectrode (CFME) and N, N'-2-pyridylethylenediamine (DPEA) which can specifically bind to Cu²⁺. The surface area and electrocatalytic performances of the system were significantly improved by AuNPs. MB-modified DNA as the internal reference substance inhibited the interference from other biological molecules and ions in brain tissue. Firstly, the peak current of Cu²⁺ coordinated with DPEA was displayed at a specific potential, which increased with the increase of Cu²⁺ concentration. The addition of CySH led to the release of Cu²⁺ for the Cu²⁺-DPEA complex and the decrease of peak current. In this process, MB-modified DNA as the built-in reference always had a constant peak current density at another potential. According to the peak current density ratio of Cu²⁺ to the internal reference molecule at different concentrations, Cu²⁺ in artificial cerebrospinal fluid (aCSF) was detected with a linear range of 1 ~ 14 μ M, and the detection limit is about 0.32 μ M. In addition, according to the peak current density ratio of CySH to internal reference molecule at different concentrations, the linear range for CySH detection is 1 ~ 12 μ M, and the detection limit is 0.48 μ M.

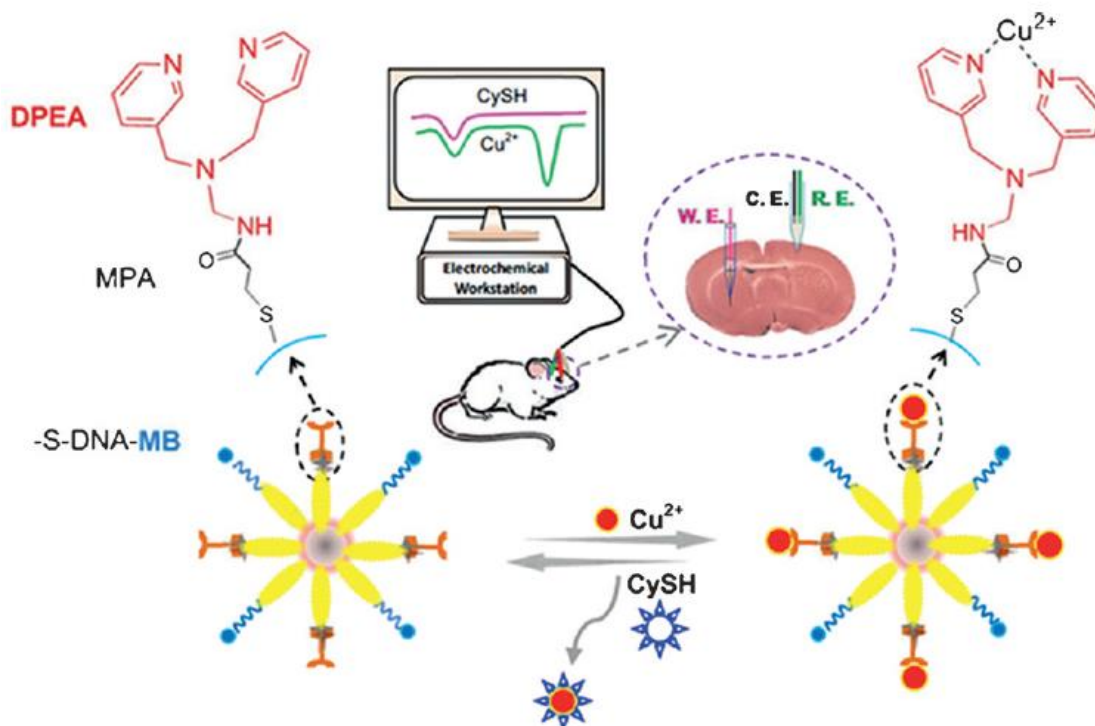


Figure 10. Illustration of the single electrochemical biosensor for in vivo ratiometric monitoring of Cu^{2+} and CySH in live rat brain with Alzheimer's Disease. Reprinted with permission from [67]. Copyright 2014 John Wiley and Sons

4. CONCLUSION

Ratiometric electrochemical biosensors can overcome the limitations of traditional single-signal electrochemical sensors (such as low sensitivity, false-positive or false-negative signals), thus improving the detection accuracy and sensitivity. In this paper, two strategies for the preparation of ratiometric electrochemical biosensors are systematically reviewed. It is worth noting that the following problems still exist in ratiometric electrochemical biosensors. For example, the types of signal labels are limited and the cost for labeling of probe is high. Therefore, the design of low-cost, simple and versatile ratiometric electrochemical biosensors will become the focus of future development in this field. By coating electrochemical active molecules with nanomaterials or in situ growth of nanomaterials with biomolecules, electrochemical biosensors with no label, low cost and high sensitivity are desired. Additionally, it is expected to realize the miniaturization and portability of ratiometric electrochemical biosensors based on screen printing technology. Dual/multiple biochemical analysis is performed in a sensing system using dual or multiple ratiometric electrochemical signal sensing modes. Finally, the application of ratiometric electrochemistry is extended to be carried out in vivo and on-line analysis.

ACKNOWLEDGEMENTS

Partial support of this work by the Natural Science Foundation of Henan Province (182300410162) was acknowledged.

References

1. X. Luo and J. J. Davis, *Chem. Soc. Rev.*, 42 (2013) 5944.
2. N. Wongkaew, M. Simsek, C. Griesche and A. J. Baeumner, *Chem. Rev.*, 119 (2019) 120.
3. M. Majdinasab, A. Hayat and J. L. Marty, *TrAC-Trend. Anal. Chem.*, 107 (2018) 60.
4. L. Liu, D. Deng, W. Sun, X. Yang, S. Yang and S. He, *Int. J. Electrochem. Sci.*, 13 (2018) 10496.
5. D. Deng, Y. Hao, S. Yang, Q. Han, L. Liu, Y. Xiang, F. Tu and N. Xia, *Sens. Actuat. B: Chem.*, 286 (2019) 415.
6. L. Liu, C. Cheng, Y. Chang, H. Ma and Y. Hao, *Sens. Actuat. B: Chem.*, 248 (2017) 178.
7. N. Xia, Z. H. Chen, Y. D. Liu, H. Z. Ren and L. Liu, *Sens. Actuat. B: Chem.*, 243 (2017) 784.
8. N. Xia, X. Wang, J. Yu, Y. Y. Wu, S. C. Cheng, Y. Xing and L. Liu, *Sens. Actuat. B: Chem.*, 239 (2017) 834.
9. L. Liu, Y. Hao, D. Deng and N. Xia, *Nanomaterials*, 9 (2019) 316.
10. N. Xia, X. Wang, B. Zhou, Y. Wu, W. Mao and L. Liu, *ACS Appl. Mater. Interfaces*, 8 (2016) 19303.
11. V. C. Diculescu, A.-M. Chiorcea-Paquim and A. M. Oliveira-Brett, *TrAC-Trend. Anal. Chem.*, 79 (2016) 23.
12. R. Gui, A. Wan, Y. Zhang, H. Li and T. Zhao, *Anal. Chem.*, 86 (2014) 5211.
13. W. Suginta, P. Khunkaewla and A. Schulte, *Chem. Rev.*, 113 (2013) 5458.
14. H. Jin, R. Gui, J. Yu, W. Lv and Z. Wang, *Biosens. Bioelectron.*, 91 (2017) 523.
15. R.-N. Ma, L.-L. Wang, H.-F. Wang, L.-P. Jia, W. Zhang, L. Shang, Q.-W. Xue, W.-L. Jia, Q.-Y. Liu and H.-S. Wang, *Sens. Actuat. B: Chem.*, 269 (2018) 173.
16. S. Xie, J. Zhang, Y. Yuan, Y. Chai and R. Yuan, *Chem. Commun.*, 51 (2015) 3387.
17. T. Yang, R. Yu, S. Liu, Z. Qiu, S. Luo, W. Li and K. Jiao, *Sens. Actuat. B: Chem.*, 267 (2018) 519.
18. X. Cai, S. Weng, R. Guo, L. Lin, W. Chen, Z. Zheng, Z. Huang and X. Lin, *Biosens. Bioelectron.*, 81 (2016) 173.
19. C. Deng, X. Pi, P. Qian, X. Chen, W. Wu and J. Xiang, *Anal. Chem.*, 89 (2017) 966.
20. F. Gao, Y. Qian, L. Zhang, S. Dai, Y. Lan, Y. Zhang, L. Du and D. Tang, *Biosens. Bioelectron.*, 71 (2015) 158.
21. K. Ikebukuro, C. Kiyohara and K. Sode, *Biosens. Bioelectron.*, 20 (2005) 2168.
22. Y. Lin, J. Jia, R. Yang, D. Chen, J. Wang, F. Luo, L. Guo, B. Qiu and Z. Lin, *Anal. Chem.*, 91 (2019) 3717.
23. K. Peng, P. Xie, Z.-H. Yang, R. Yuan and K. Zhang, *Biosens. Bioelectron.*, 102 (2018) 282.
24. S. A. Spring, S. Goggins and C. G. Frost, *Org. Biomol. Chem.*, 15 (2017) 7122.
25. Y. Wei, H. Ma, X. Ren, C. Ding, H. Wang, X. Sun, B. Du, Y. Zhang and Q. Wei, *Sens. Actuat. B: Chem.*, 256 (2018) 504.
26. S. Yang, F. Zhang, Q. Liang and Z. Wang, *Biosens. Bioelectron.*, 120 (2018) 85.
27. D. Yao, W. Zhao, L. Zhang and Y. Tian, *Analyst*, 142 (2017) 4215.
28. J. Yu, H. Jin, R. Gui, W. Lv and Z. Wang, *J. Electroanal. Chem.*, 795 (2017) 97.
29. P. Yu, X. Zhang, J. Zhou, E. Xiong, X. Li and J. Chen, *Sci. Rep.*, 5 (2015) 16015.
30. C. Zhao, H. Jin, R. Gui and Z. Wang, *Sens. Actuat. B: Chem.*, 242 (2017) 71.
31. C. Zhu, M. Liu, X. Li, X. Zhang and J. Chen, *Chem. Commun.*, 54 (2018) 10359.
32. K. Ren, J. Wu, F. Yan, Y. Zhang and H. Ju, *Biosens. Bioelectron.*, 66 (2015) 345.
33. D. Deng, L. Liu, Y. Bu, X. Liu, X. Wang and B. Zhang, *Sens. Actuat. B: Chem.*, 269 (2018) 189.

34. L. Cui, M. Lu, X. Yang, B. Tang and C. Zhang, *Analyst*, 142 (2017) 1562.
35. Q. Pu, J. Li, J. Qiu, X. Yang, Y. Li, D. Yin, X. Zhang, Y. Tao, S. Sheng and G. Xie, *Biosens. Bioelectron.*, 94 (2017) 719.
36. Y. H. Yuan, B. Z. Chi, S. H. Wen, R. P. Liang, Z. M. Li and J. D. Qiu, *Biosens. Bioelectron.*, 102 (2018) 211.
37. J. Zhang, L. L. Wang, M. F. Hou, Y. K. Xia, W. H. He, A. Yan, Y. P. Weng, L. P. Zeng and J. H. Chen, *Biosens. Bioelectron.*, 102 (2018) 33.
38. E. Xiong, Z. Li, X. Zhang, J. Zhou, X. Yan, Y. Liu and J. Chen, *Anal. Chem.*, 89 (2017) 8830.
39. L. Ge, W. Wang and F. Li, *Anal. Chem.*, 89 (2017) 11560.
40. P. Gai, C. Gu, H. Li, X. Sun and F. Li, *Anal. Chem.*, 89 (2017) 12293.
41. H. R. Zhang, J. J. Xu and H. Y. Chen, *Anal. Chem.*, 85 (2013) 5321.
42. X. Liu, Z. Yan, Y. Sun, J. Ren and X. Qu, *Chem. Commun.*, 53 (2017) 6215.
43. E. Xiong, X. Zhang, Y. Liu, J. Zhou, P. Yu, X. Li and J. Chen, *Anal. Chem.*, 87 (2015) 7291.
44. N. Hao, X. L. Li, H. R. Zhang, J. J. Xu and H. Y. Chen, *Chem. Commun.*, 50 (2014) 14828.
45. X. Li, B. Dou, R. Yuan and Y. Xiang, *Sens. Actuat. B: Chem.*, 286 (2019) 191.
46. B. Dou, J. Li, B. Jiang, R. Yuan and Y. Xiang, *Anal. Chim. Acta*, 1038 (2018) 166.
47. L. Liu, Y. Gao, H. Liu and N. Xia, *Sens. Actuat. B-Chem.*, 208 (2015) 137.
48. L. Liu, N. Xia, H. Liu, X. Kang, X. Liu, C. Xue and X. He, *Biosens. Bioelectron.*, 53 (2014) 399.
49. N. Xia, K. Liu, Y. Zhou, Y. Li and X. Yi, *Int. J. Nanomed.*, 12 (2017) 5013.
50. L. Liu, Y. Chang, J. Yu, M. Jiang and N. Xia, *Sens. Actuat. B: Chem.*, 251 (2017) 359.
51. L. Cui, M. Lu, Y. Li, B. Tang and C. Y. Zhang, *Biosens. Bioelectron.*, 102 (2018) 87.
52. L. Wang, C. Gong, Y. Shen, W. Ye, M. Xu and Y. Song, *Sens. Actuat. B: Chem.*, 242 (2017) 625.
53. J. Yu, H. Jin, R. Gui, Z. Wang and F. Ge, *Talanta*, 162 (2017) 435.
54. X. Zhang, L. Wu, J. Zhou, X. Zhang and J. Chen, *J. Electroanal. Chem.*, 742 (2015) 97.
55. H. Cheng, X. Wang and H. Wei, *Anal. Chem.*, 87 (2015) 8889.
56. C. Gong, Y. Shen, Y. Song and L. Wang, *Electrochim. Acta*, 235 (2017) 488.
57. K. Manibalan, V. Mani, P. C. Chang, C. H. Huang, S. T. Huang, K. Marchlewicz and S. Neethirajan, *Biosens. Bioelectron.*, 96 (2017) 233.
58. W. J. Shen, Y. Zhuo, Y. Q. Chai and R. Yuan, *Anal. Chem.*, 87 (2015) 11345.
59. Q. Xu, Z. Liu, J. Fu, W. Zhao, Y. Guo, X. Sun and H. Zhang, *Sci. Rep.*, 7 (2017) 14729.
60. S. Goggins, E. A. Apey, M. F. Mahon and C. G. Frost, *Org. Biomol. Chem.*, 15 (2017) 2459.
61. Y. Wang, G. Ning, H. Bi, Y. Wu, G. Liu and Y. Zhao, *Electrochim. Acta*, 285 (2018) 120.
62. Y. Song, M. Xu, C. Gong, Y. Shen, L. Wang, Y. Xie and L. Wang, *Sens. Actuat. B: Chem.*, 257 (2018) 792.
63. X. Li and X. Kan, *Analyst*, 143 (2018) 2150.
64. Z. Qiu, T. Yang, R. Gao, G. Jie and W. Hou, *J. Electroanal. Chem.*, 835 (2019) 123.
65. J. Jia, H. G. Chen, J. Feng, J. L. Lei, H. Q. Luo and N. B. Li, *Anal. Chim. Acta*, 908 (2016) 95.
66. Y. Yu, C. Yu, T. Yin, S. Ou, X. Sun, X. Wen, L. Zhang, D. Tang and X. Yin, *Biosens. Bioelectron.*, 87 (2017) 278.
67. Y. Luo, L. Zhang, W. Liu, Y. Yu and Y. Tian, *Angew. Chem. Int. Ed.*, 54 (2015) 14053.
68. X. Chai, X. Zhou, A. Zhu, L. Zhang, Y. Qin, G. Shi and Y. Tian, *Angew. Chem. Int. Ed.*, 52 (2013) 8129.
69. L. Zhang, Y. Han, F. Zhao, G. Shi and Y. Tian, *Anal. Chem.*, 87 (2015) 2931.
70. Y. Yu, P. Wang, X. Zhu, Q. Peng, Y. Zhou, T. Yin, Y. Liang and X. Yin, *Analyst*, 143 (2018) 323.
71. X. Chai, L. Zhang and Y. Tian, *Anal. Chem.*, 86 (2014) 10668.
72. P. Huang, F. Wu and L. Mao, *Anal. Chem.*, 87 (2015) 6834.
73. Y. Cheng, Y. Huang, J. Lei, L. Zhang and H. Ju, *Anal. Chem.*, 86 (2014) 5158.
74. F. Zhao, L. Zhang and A. Zhu, *Chem. Commun.*, 52 (2016) 3717.
75. X. Yu, Z. Wang, Y. Gao, F. Kong, W. Lv, H. Ma and W. Wang, *Int. J. Electrochem. Sci.*, 13 (2018) 2875.

76. N. Xia, B. Zhou, N. Huang, M. Jiang, J. Zhang and L. Liu, *Biosens. Bioelectron.*, 85 (2016) 625.

© 2019 The Authors. Published by ESG (www.electrochemsci.org). This article is an open access article distributed under the terms and conditions of the Creative Commons Attribution license (<http://creativecommons.org/licenses/by/4.0/>).